Development of a Linear-Source, Atmospheric-Pressure RF Glow Discharge Plasma

Andrew J. Wagner, *Student Member, IEEE*

Abstract—**A linear-source, atmospheric-pressure RF glow discharge plasma has been designed, fabricated, and analyzed. The RIT atmospheric-pressure plasma (RITAPP) consists of two parallel-plate electrodes separated by a 1.2 mm gap. Helium is flown through the gap, exiting the slit and impinging a substrate. 13.56 MHz RF power is applied to one electrode, resulting in a non-thermal plasma with a gas temperature (T_g) between 50 and 150 °C. Optical emission spectroscopy was used to determine spectral radiation in the UV-Vis region of helium and helium/oxygen plasmas. Singlet and triplet helium emissions as well as numerous O, H, and OH peaks are observed. Surface treatment of bare 2" (100) p-type silicon wafers was performed by short exposure to a He/O_2 plasma exposure increased surface energy, creating a hydrophilic surface. 20-minute exposures of bare and RCA-cleaned silicon substrates to a He/O_2 plasma were analyzed using ellipsometry and mercury probe C-V measurements. Optical thickness was determined to be 3.4 nm while C-V measurements revealed that both the plasma-grown oxide and the chemical oxides exhibited enhanced dielectric properties following treatment. Work is ongoing to expand upon oxidation experiments as well as I-V diagnostics of the plasma. In addition, investigation of low-temperature carbon nanotube growth is underway.**

Index Terms—**Atmospheric, Glow Discharge, Oxide, Plasma, Radio Frequency, Surface Treatment**

I. Introduction

LOW-PRESSURE plasmas have long been utilized in materials processing. These plasmas offer high concentrations of chemically reactive species at low gas temperatures while maintaining a uniform gradient of reactive species over a large area. This makes them ideal for etching, deposition, and surface treatment [1]. Unfortunately, low-pressure plasmas are limited by their requirement for expensive vacuum systems which require continued maintenance, and limit the size and throughput of treated substrates. High-pressure (e.g. atmospheric) plasmas pose an impressive advantage over their low-pressure counterparts, as the need for vacuum systems is eliminated. This opens the door for the exploration of new processing environments, including open air.

Atmospheric-pressure, high-temperature plasmas (e.g. torches and plasma spray [2]) are common in applications where substrates are not thermally sensitive or the exposure time is kept very short. Low-temperature, atmospheric-pressure plasmas, such as the corona discharge and the dielectric barrier discharge (DBD), have been utilized in recent decades for surface treatment applications. A major limitation of these systems is that they are not uniform throughout the discharge volume (non-homogeneous) and have relatively low electron densities when averaged over time and space. This can make them useful for surface treatment, but etching and thin film deposition capabilities are limited.

Recently, homogeneous atmospheric-pressure plasmas (APP), also called atmospheric-pressure glow discharges (APGD), operating at low temperature have been realized [3-6]. These offer many of the benefits of low-pressure plasmas without the drawbacks of a vacuum environment or the uniformity issues of other atmospheric-pressure plasmas. Compared to low-pressure plasma deposition tools, APP offers reduced up front costs through elimination of vacuum, reduced cost of ownership through reduced maintenance, improved throughput, and can potentially be applied to any size substrate. In this paper RIT's proof of concept atmospheric-pressure plasma deposition tool is described. Development of the RIT atmospheric-pressure plasma (RITAPP) system is discussed. Plasma diagnostics are then examined using optical and thermal spectroscopic analysis. Finally, preliminary application studies for surface treatment and silicon dioxide growth explored.

II. Theory

A. What is plasma?

Plasmas are ionized gases, often referred to as the fourth state of matter, which constitute an estimated 99% of the matter in the universe. They contain positive and negative ions, neutral species, and electrons. Plasma is generally electrically neutral; however, it contains free charge carriers and is electrically conductive. Plasmas are often referred to as partially- or fully-ionized, which refers to the degree of ionization in the gas. The RITAPP is a weakly ionized plasma, where only a small fraction of the atoms are ionized *[3, 5]*.

B. Creation of Plasma

Plasma is created when energy is provided to a gas. This energy can be either thermal or supplied by an electric field or

Manuscript received May 21, 2008. This work was supported in part by the Rochester Institute of Technology (Rochester, NY), MKS Instruments (Rochester, NY), and Applied Materials (Santa Clara, CA).

A. J. Wagner is with Rochester Institute of Technology, Rochester, NY 14623 USA (phone: 585-217-2711; e-mail: ajw8557@rit.edu).

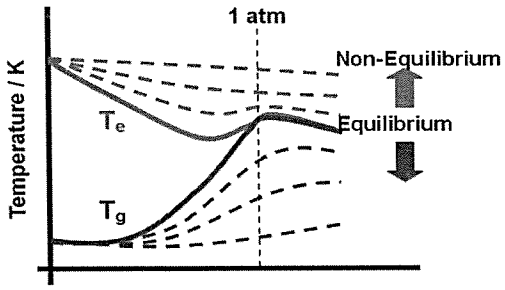

Fig. 1. Electron and gas temperature in plasmas with respect to pressure. As pressure increases over 1 atmosphere, the electron and gas temperatures equilibrate. For non-thermal plasma at high pressure, certain methods can be implemented to create a disparity between the two temperatures.

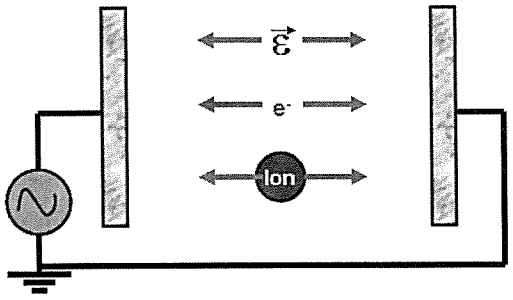

Fig. 2. Schematic of parallel plate configuration of an rf glow discharge plasma. During each half cycle of the applied bias, electrons are accelerated against the electric field while positive ions accelerate in the direction of the field. The short duration of each half cycle allows electrons to gain enough kinetic energy to ionize the gas, however heavy particles remain in a non-equilibrium state with respect to the electron temperature.

electromagnetic radiation. Under an applied electric field, electrons in the gas are accelerated. The electrons collide with neutral species, modifying the electronic structure of the neutral species, creating excited species, ions and more electrons [3, 7, 8].

C. *Thermal versus Non-Thermal Plasmas*

Atmospheric-pressure plasmas, such as welders and torches, are thermal in nature. These plasmas are at or near equilibrium where the electrons, ions, and neutrals have the same temperature. As pressure is reduced, the number of elastic collisions between heavy particles decrease, creating a disparity between the temperatures of the electrons and the gas and giving rise to a non-thermal plasma, as seen in Figure 1. For a low-temperature plasma at high pressure, methods must be implemented to force a non-equilibrium condition between the electron and gas temperatures [1, 3, 7, 8].

D. *Non-Thermal Atmospheric Plasmas*

1) *Dielectric Barrier Discharge*

The DBD makes use of a dielectric barrier on one or more of the electrodes, preventing charges created in the gas from reaching the electrodes. Due to the dielectric barrier, no DC current can be passed and an AC bias must be applied. When the applied AC bias exceeds a breakdown voltage, narrow discharge filaments conduct electrons through the gap and towards the more positive electrode. As charge buildup occurs on the dielectric barrier, the voltage drop across the filament is reduced until it can no longer be sustained and the discharge is extinguished. These microdischarges last on the nanosecond time scale while heavy particle reactions require a duration orders of magnitude higher to reach equilibrium.

While the DBD has been used for over a century in various applications, the filamentary nature of the plasma limits its application. The non-homogeneous nature in both space and time creates non-uniformities on a scale too large for materials processing requiring uniform treatment such as in microelectronics [3, 9].

2) *RF Glow Discharge*

Glow discharge plasmas at atmospheric pressure make use an RF bias applied to one of two capacitively coupled, bare-metal electrodes spaced a few millimeters apart, as shown in Figure 2. The RF bias results in an electric field capable of accelerating electrons on each half cycle and giving them enough kinetic energy to, upon collision with a heavy particle, cause ionization. The resultant ions under the same bias are unable to gain enough kinetic energy to equilibrate gas.

Unlike the DBD, the discharge maintained under an applied bias is homogeneous and free of filaments or arcs. The gas temperature remains on the order of 300-500 K while the electron temperature can exceed 10000 K [3, 6, 9, 10].

III. Development of the RIT Atmospheric-Pressure Plasma

A. *Plasma Head*

A linear-source plasma is ideal for potential scaling to large areas. Such a design requires a wide, thin gap contained between a powered and a grounded electrode across which an electric potential is applied. In this gap, an easily ionized gas is flown. When the electric field is applied, the gas between the electrodes ionizes, forming a capacitively coupled plasma. Helium (Airgas, 99.999% purity) was chosen for initial study due to its low breakdown voltage and electrical stability under moderate power [11]. A sufficiently small gap is required in order to allow a high enough electric field for breakdown of the working gas. Prior work has shown that a gap on the order of 1 – 2 mm is appropriate [10]. All work herein uses a 1.2 mm gap.

The RITAPP plasma head, Figure 3, was designed so that the gap may be changed by using different spacers. Powered electrode area was limited to keep power requirements to a minimum while still realizing a useful plasma size. The electrode material has negligible effect on the plasma properties due to the weak ion bombardment in the atmospheric pressure [12]. Aluminum was chosen as the electrode material for its high conductivity and ease of machining. A two-inch wide slit was chosen for complete coverage of a two-inch silicon wafer, resulting in a powered electrode 50.8 mm wide by 50.8 mm long.

In addition to plasma size considerations, a uniform treatment of a substrate requires that gas flow exiting the plasma head be homogeneous across the width of the slit. For this, computational fluid dynamics (CFD) simulations were performed using COSMOSFloWorks, as seen in Figure 4,

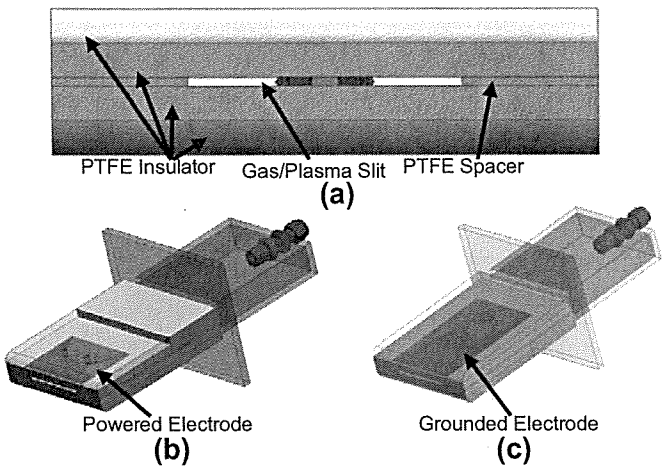

Fig. 3. 3-D Schematic of the RITAPP plasma head. (a) Looking into bottom of plasma head. (b) and (c) isometric views. Electrodes are made of aluminum and encapsulated on all sides not facing gap by Teflon for electrical insulation. A gas diffusion box is placed at entrance of slit to provide area for mixing of gases.

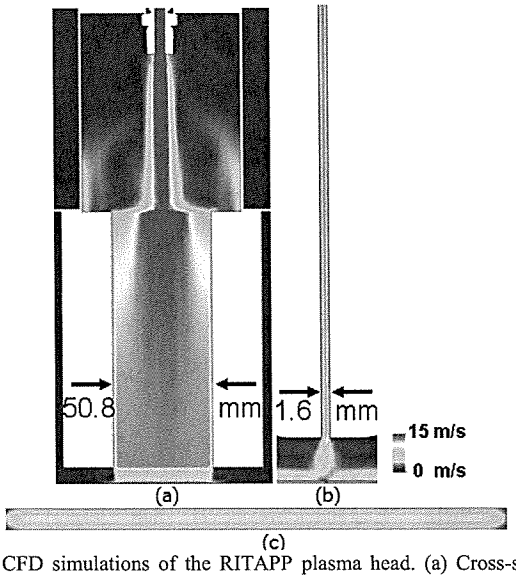

Fig. 4. CFD simulations of the RITAPP plasma head. (a) Cross-sectional view parallel to electrodes in center of gap. (b) Cross-sectional view normal to electrodes in center of gap. (c) Cross-sectional view looking into end of slit. Gas exiting slit is fully developed, allowing uniform exposure of the substrate to the plasma effluent.

assuming a 50 sLm flow of helium and oxygen, to confirm uniform velocity exiting the slit. High flows, correlating to velocities between 5 and 12 m/s, ensure that no outside air enters the plasma slit. The large "diffusion" gas box prior to entry of gas into the slit allows for mixing of gases and room to add diffusion barriers for gas mixing if needed.

The final plasma head design can be seen in Figure 5. Two aluminum plates were used to compress the insulators, spacers, and electrodes together. These plates were then attached to the diffuser box to seal the plasma head. The powered electrode was attached to a Type N connector while the grounded electrode was connected to the plasma head body.

B. Impedance Matching Network

Inherent in any RF design is the complex impedance of the plasma head. RF power sources are designed to see a 50 Ω

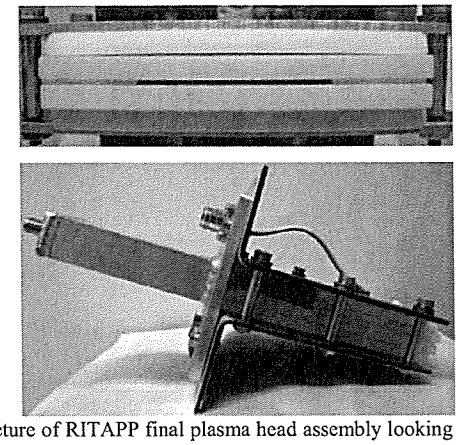

Fig. 5. Picture of RITAPP final plasma head assembly looking into slit (top) and isometric view (bottom). Compressive plates can be seen holting insulators, electrodes, and spacers together. Connected to the plates is the gas diffuser box, completing the plasma head assembly. A Type N connector is used to connect electrodes to the matchwork.

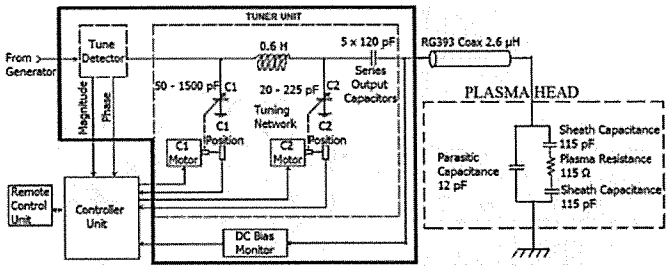

Fig. 6. CFD simulations of the RITAPP plasma head. (a) Cross-sectional view parallel to electrodes in center of gap. (b) Cross-sectional view normal to electrodes in center of gap. (c) Cross-sectional view looking into end of slit. Gas exiting slit is fully developed, allowing uniform exposure of the substrate to the plasma effluent.

load. Any deviation from this impedance results in reflected power, putting stress on the source and requiring additional power input to power the plasma. Working with a senior engineer at MKS Instruments (Rochester, NY), an impedance matching network (matchwork) was designed (Figure 6). The matchwork is a modified ENI MWH-5 automated tunable matchwork consisting of a pi-network with two variable capacitors, an inductor, and a load capacitor. The variable capacitors are attached to motors that are varied by a control unit. The control unit determines optimal capacitance through an electrical phase and magnitude "phase/mag" detector at the input of the matchwork. In order to determine the appropriate capacitors and inductors, the impedance of the plasma was calculated. Based on previous work [6], in addition to capacitance calculations, a plasma equivalent circuit was created. MathCAD was then used to calculate the impedance of the entire circuit (matchwork and plasma equivalent circuit) and the variable capacitor range that would give the largest tunable range. The resultant allowable load impedance range can be seen on the Smith chart in Figure 7. Upon completion of the modified MWH-5, the unit was tested at low power using an Agilent E5071C network analyzer and determined to be capable of providing an accurate tune with an impedance of 50.203 – j0.074 Ω and a standing wave ratio of 1.09.

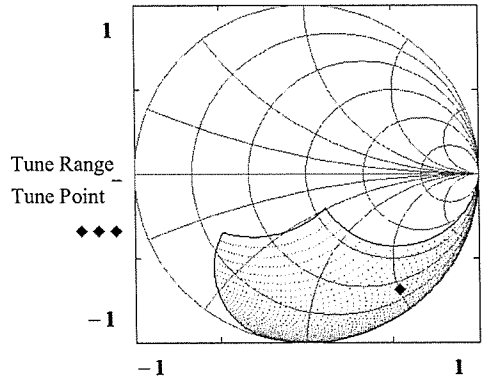

Fig. 7. Smith chart indicating tune range of the impedance matching network. The calculated impedance of the plasma is the black diamond while the matchwork's tunable range is within the dotted area.

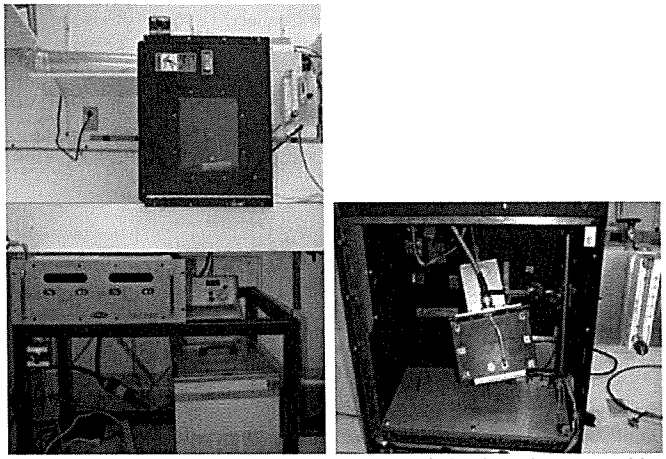

Fig. 8. Smith chart indicating tune range of the impedance matching network. The calculated impedance of the plasma is the black diamond while the matchwork's tunable range is within the black line.

C. System Setup

The RITAPP plasma head is placed in an exhaust chamber for removal of effluent gases, as seen in Figure 8. A Comdel DX-2000 RF source (courtesy: Applied Materials) is attached to the matchwork and then connected to the plasma head within the chamber. A hotplate underneath the plasma head is used for heating of substrates during processing.

IV. RITAPP Diagnostics

A. First Plasma

Plasma was achieved by flowing helium between 15 and 50 sLm between the electrodes spaced 1.2 mm apart. 13.56 MHz RF power between 20 and 130 W was applied to the powered electrode, corresponding to a maximum power density of 5 W/cm^2. Power over 130 W resulted in arcing between the electrodes. Pictures of the discharge can be seen in Figure 9, taken with a Nikon D50 and a 15-55mm lens.

Additional investigation of He/O_2 (Airgas 99.999% purity) plasmas determined that a glow discharge can be sustained with oxygen making up less than 3 %vol of the gas. Emission intensity decreased as a result of the addition of oxygen, however power density reached 8 W/cm^2 (200 W applied) was reached before arcing. A comparison of a He and a He/O_2 plasma can be seen in Figure 10. Images were taken using a Nikon camera with a baffle and thimble lens.

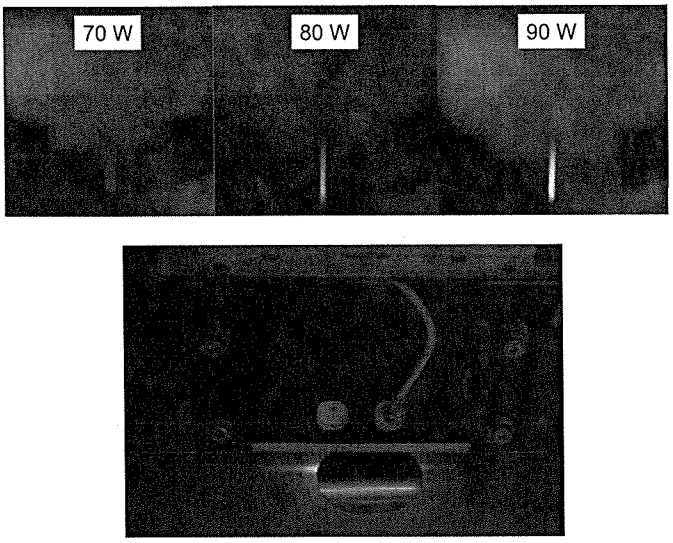

Fig. 9. Pictures of helium glow discharges from the RITAPP plasma head impinging a 2" silicon wafer. (a) 70 W, 50 sLm helium plasma. (b) 80 W, 50 sLm helium plasma. (c) 80 W, 50 sLm helium plasma. (d) 80 W, 50 sLm helium plasma.

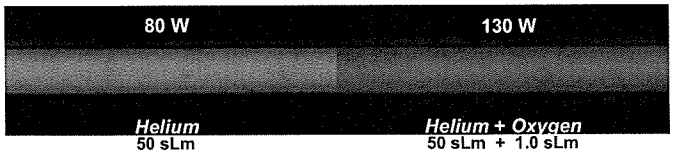

Fig. 10. Comparison of helium and helium/oxygen discharges. The He discharge appears blue to the human eye while the He/O2 discharge appears white. Even at higher power densities the He/O2 plasma has lower emission.

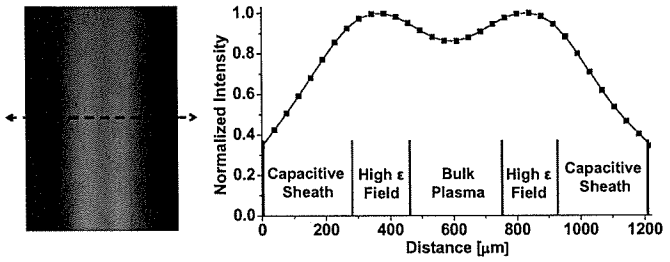

Fig. 11. Emission intensity profile of an 80 W, 50 sLm helium plasma in a 1.2 mm gap. Discharge near the electrodes is low due to the electron-depleted capacitive ion sheaths. Emission peaks just outside of the sheaths where electric field is highest, leveling off in the bulk plasma.

B. Plasma Emission Intensity Profile

A photograph across the discharge, as seen in Figure 11, was taken for analysis of emission intensity profile. Variable spatial emission between the electrodes is observed – a result of capacitive sheaths adjacent to the electrodes. These space charge sheaths are a result of a net imbalance between ion and electron densities near the electrodes. This imbalance creates a local electric field which accelerates ions towards the electrodes and electrons into the bulk [13].

As a result of the low electron density, few excitation collisions occur within the sheaths, resulting in low emission. High electric field on the sheath edge results in higher emission at the edge of the bulk than in the center.

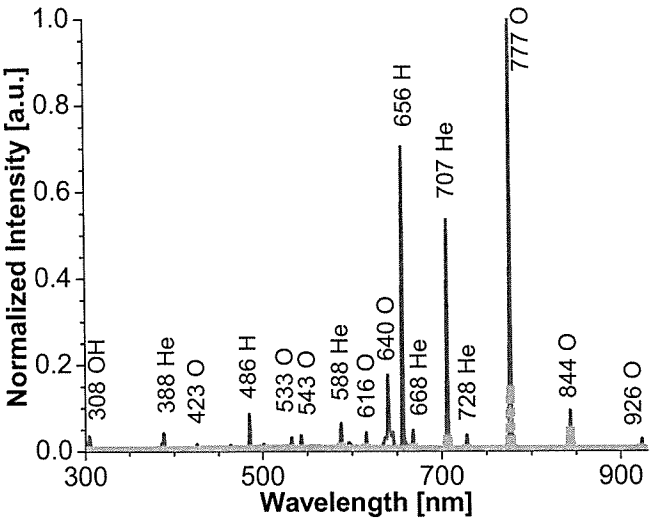

Fig. 12. Optical emission spectroscopy of a 70 W, 50 sLm helium plasma (black) and a 70 W, 50 sLm helium + 1.5 sLm oxygen plasma (gray). Emission is much lower in the He/O_2 plasma due to an increase in breakdown voltage to sustain the plasma, decreasing current for the same power. Addition of oxygen nearly doubles attainable input power.

C. *Optical Emission Spectroscopy*

In order to determine excited species, optical emission spectroscopy (OES) (Ocean Optics HR4000, HC-1 grating) was utilized. Comparison of the emission of a 70 W helium and a 70 W helium/oxygen plasma can be seen in Figure 12. Emission intensity is substantially decreased in the oxygen plasma – likely a result of the higher breakdown voltage required. For the same power, lower current can be achieved. Numerous hydrogen, oxygen, and hydroxyl peaks are observed in the pure helium plasma, indicating water contamination. Efforts to determine the source of contamination are ongoing.

Time resolved OES of a helium plasma, Figure 13, revealed an increase in emission intensity with respect to time. Effluent gas temperature was measured with a Type T thermocouple placed 3 mm downstream of the electrodes over the same time and was seen to increase, reaching a maximum of 372 K. It is believed that heating of the electrodes leads to heating of the gas and emission intensity.

D. *Determination of Non-Equilibrium Condition*

The simplest model for a plasma is based on the Maxwell-Boltzmann distribution. This model, however, assumes an equilibrium plasma and is not suited for non-thermal plasmas. Nevertheless, application of the Boltzmann model to excitation temperature of atomic species in the discharge (1) can be used to determine whether the plasma is in an equilibrium state. The excitation temperature of an excited atom is

$$T = \frac{E_i - E_j}{k} \frac{1}{\ln\left(\frac{I_{ik}}{I_{jh}} \frac{\nu_j}{\nu_i} \frac{A_j}{A_i} \frac{g_j}{g_i}\right)} \quad (1)$$

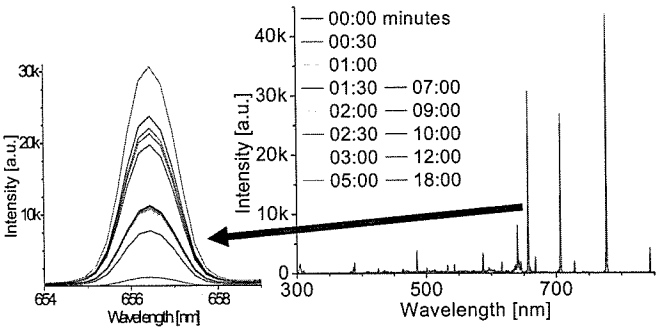

Fig. 13. Optical emission spectroscopy of a 70 W, 50 sLm helium plasma with respect to time. Increase in the emission intensity is observed over time. Measurements of effluent gas temperature indicate a correlated increase in temperature – likely due to heating of the electrodes.

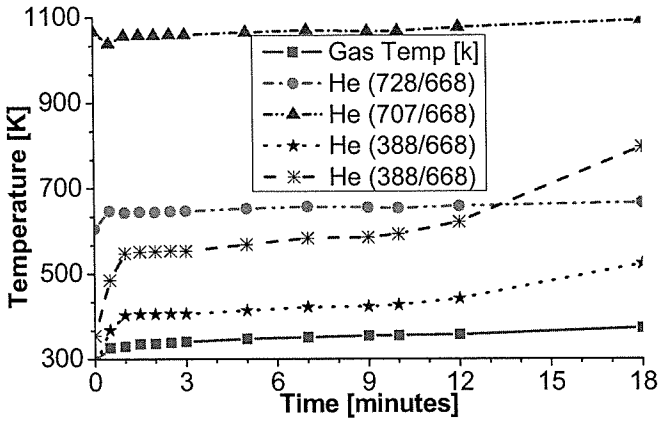

Fig. 14. Excitation temperatures with respect to time of a 70 W, 50 sLm helium plasma. Distribution of temperatures, all over the gas temperature, confirms the non-thermal nature of the RITAPP.

where T is excitation temperature, E is the upper level energy of an excited atom, I is the relative emission intensity, ν is the emission frequency, A is the transition probability, and g is the statistical weight. The latter three variables are obtained from the NIST atomic spectra database [14].

If the plasma is at or near equilibrium, the excitation temperatures should match. A distribution of excitation temperatures (notably from the gas temperature) supplies evidence of a non-thermal plasma. Using the emission profile of the helium plasma in Figure 13, excitation temperatures were found with respect to time, as seen in Figure 14. The distribution of excitation energies, all of which are above the effluent gas temperature, confirm that the RITAPP a non-thermal atmospheric-pressure plasma.

V. Atmospheric Pressure Plasma Applications

A. *Surface Treatment*

Capability of surface treatment using the RITAPP was performed on hydrophobic (100)-Si wafers. The substrates were RCA cleaned with a final 50:1 HF dip to remove the chemical oxide and exposed to a He/O_2 plasma. Contact angle measurement revealed increased surface energy, making the wafer hydrophilic, as seen in Figure 15.

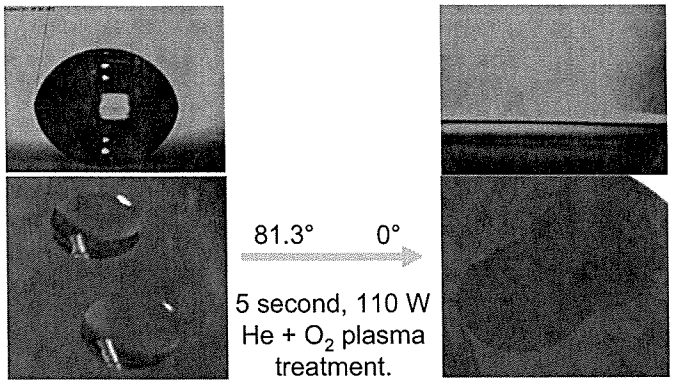

Fig. 15. Surface modification of a clean, bear silicon wafer. Following an RCA clean and 50:1 HF dip, the contact angle between water and the substrate was 81.3°. After a short exposure to a helium/oxygen plasma, wetting resulted in no measurable contact angle.

The plasma creates ionized molecular oxygen and radical atomic oxygen, which react with material and result in higher surface energy. Such a process is ideal for applications such as improved anodic bonding, textile treatment, and thin film adhesion promotion.

B. Silicon Dioxide Growth/Modification

Using a helium/oxygen plasma, silicon dioxide growth on bare (100)-Si substrates and (100)-Si substrates with a chemical oxide from an RCA clean was attempted. Analysis was performed using an ellipsometer (J.A. Woollam VASE) and a mercury probe capacitance-voltage tool (MDC). Optical and electrical thickness measurements do not agree, but both indicate oxide growth. C-V curves for samples not exposed to the plasma indicate poor dielectric properties. Dielectric properties of the samples exposed to the plasma were enhanced. Bare samples exhibit high hysteresis and interface traps, while those from the chemical oxide samples appear to be greatly enhanced.

VI. Conclusion

A non-thermal, atmospheric-pressure glow discharge plasma has been successfully designed, fabricated, and tested. Helium is flown between two bare metal electrodes separated by a 1.2 mm gap at velocities between 5 and 12 m/s. RF power between 20 and 200 W is applied to one electrode, generating a glow discharge plasma. Gas temperature of the plasma effluent was between 50 and 150 °C. Surface modification has been demonstrated on bare silicon exposed to a He/O_2 plasma. Exposure increased surface energy of the film. Oxides with optical thicknesses of 30 nm have been grown. Exposure of chemical oxides to the plasma enhanced their dielectric properties. The RITAPP system shows promise as a tool for low-temperature, atmospheric-pressure materials processing. Work is ongoing to characterize the plasma, investigate carbon nanotube growth at low temperature, and explore potential new applications.

TABLE I
Oxide Growth Parameter Space

Treatments								Analysis			
Run	Clean Process	Power [W]	Flow [sLm] He	Flow [sLm] O_2	Time [min]	Working Distance [mm]	Substrate Temp [C]	Thickness [A] Optical	Thickness [A] Electrical	N_{ox} [cm^{-2}]	N_{ss} [cm^{-2}]
1	RCA + HF	-	-	-	-	-	-	12	N/A	N/A	N/A
2	RCA	-	-	-	-	-	-	16	N/A	N/A	N/A
3	RCA	-	-	-	20	-	340	16	N/A	N/A	N/A
4	RCA	100	50	1.5	20	6	340	31	244	$2.2x10^{15}$	$8.8x10^{10}$
5	RCA	100	50	1.5	10	34	340	20	167	$2.6x10^{14}$	$4.1x10^{11}$
6	RCA + HF	100	17	0.6	20	6	340	36	296	$4.6x10^{15}$	$6.9x10^{11}$

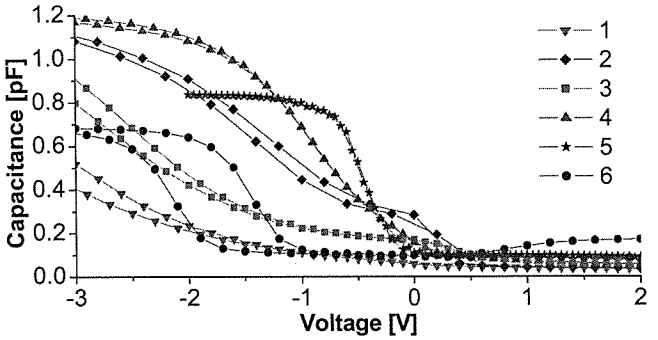

Fig. 16. Surface modification of a clean, bear silicon wafer. Following an RCA clean and 50:1 HF dip, the contact angle between water and the substrate was 81.3°. After a short exposure to a helium/oxygen plasma, wetting resulted in no measurable contact angle.

Acknowledgment

The author would like to thank his research advisor, Dr. Davide Mariotti, and academic advisor, Dr. Sean Rommel, for their support, guidance, and patience in the realization of this work. Special thanks go to Dr. Doug Schulz and Rob Sailer at the Center for Nanoscale Science & Engineering (CNSE) at North Dakota State University (NDSU) for creating the author's interest and understanding of plasma physics and thin film deposition. Additional thanks go to the staff of the Semiconductor & Microsystems Fabrication Laboratory at RIT for their never-ending hard work in the aid of this project.

References

[1] M. A. Lieberman and A. J. Lichtenberg, *Principles of Plasma Discharges and Materials Processing*: John Willey & Sons Inc, 2005.

[2] A. Gurav, T. Kodas, T. Pluym, and Y. Xiong, "AEROSOL PROCESSING OF MATERIALS," *Aerosol Science and Technology,* vol. 19, pp. 411-452, Nov 1993.

[3] C. Tendero, C. Tixier, P. Tristant, J. Desmaison, and P. Leprince, "Atmospheric pressure plasmas: A review," *Spectrochimica Acta - Part B Atomic Spectroscopy,* vol. 61, pp. 2-30, 2006.

[4] H.-B. Wang, W.-T. Sun, H.-P. Li, C.-Y. Bao, and X.-Z. Zhang, "Characteristics of radio-frequency, atmospheric-pressure glow discharges with air using bare metal electrodes," *Applied Physics Letters,* vol. 89, p. 161502, 2006.

[5] A. Bogaerts, E. Neyts, R. Gijbels, and J. Van der Mullen, "Gas discharge plasmas and their applications," *Spectrochimica Acta - Part B Atomic Spectroscopy,* vol. 57, pp. 609-658, 2002.

[6] J. Laimer, S. Haslinger, W. Meissl, J. Hell, and H. Stori, "Investigation of an atmospheric pressure radio-frequency capacitive plasma jet," *Vacuum,* vol. 79, pp. 209-214, 2005.

[7] H. Conrads and M. Schmidt, "Plasma generation and plasma sources," *Plasma Sources Science and Technology,* vol. 9, pp. 441-454, 2000.

[8] K. H. Becker, *Non-Equilibrium Air Plasmas at Atmospheric Pressure*: Institute of Physics Publishing, 2005.

[9] A. Schutze, J. Y. Jeong, S. E. Babayan, J. Park, G. S. Selwyn, and R. F. Hicks, "Atmospheric-pressure plasma jet: A review and comparison to other plasma sources," *IEEE Transactions on Plasma Science,* vol. 26, pp. 1685-1694, 1998.

[10] J. Park, I. Henins, H. W. Herrmann, G. S. Selwyn, J. Y. Jeong, R. F. Hicks, D. Shim, and C. S. Chang, "An atmospheric pressure plasma source," *Applied Physics Letters,* vol. 76, pp. 288-290, 2000.

[11] P. Jaeyoung, I. Henins, H. W. Herrmann, and G. S. Selwyn, "Gas breakdown in an atmospheric pressure radio-frequency capacitive plasma source," *Journal of Applied Physics,* vol. 89, pp. 15-19, 2001.

[12] W.-C. Zhu, B.-R. Wang, Z.-X. Yao, and Y.-K. Pu, "Discharge characteristics of an atmospheric pressure radio-frequency plasma jet," *Journal of Physics D: Applied Physics,* vol. 38, pp. 1396-1401, 2005.

[13] P. Jaeyoung, I. Henins, H. W. Herrmann, G. S. Selwyn, and R. F. Hicks, "Discharge phenomena of an atmospheric pressure radio-frequency capacitive plasma source," *Journal of Applied Physics,* vol. 89, pp. 20-8, 2001.

[14] Y. Ralchenko, F. C. Jou, D. E. Kelleher, A. E. Kramida, A. Musgrove, J. Reader, W. L. Wiese, and K. Olsen, "NIST Atomic Spectra Database (2005)(version 3.1. 2)."

Andrew J. Wagner was born in Edina, MN in 1985. He received a B.S. degree in microelectronic engineering from the Rochester Institute of Technology, May 2008, and will begin pursuit of a Ph.D. in materials science from the University of Minnesota in August 2008.

He joined Micron Technology in Boise, ID during the summer/fall in 2005 as a co-op student working in the redistribution-lithography group working on development of graytone lithography for a metal redistribution layer. During the summer/fall of 2006, he returned to Micron in the R&D Parametrics group, correlating test structures between metal levels and documenting the test structures on next-generation NAND flash. In the spring/summer of 2007, he performed research at the Center for Nanoscale Science and Engineering (CNSE) and North Dakota State University (NDSU) on the deposition of transparent conducting oxides by an atmospheric-pressure plasma jet.